How to cite: *Angew. Chem. Int. Ed.* **2023,** *62,* e202303204
doi.org/10.1002/anie.202303204

Zeolites Hot Paper

Spectroscopic Signatures of Internal Hydrogen Bonds of Brønsted-Acid Sites in the Zeolite H-MFI

Henning Windeck[+]*, Fabian Berger*[+]*, and Joachim Sauer**

Abstract: The location of Brønsted-acid sites (bridging OH groups, b-OH) at different crystallographic positions of zeolite catalysts influences their reactivity due to varying confinement. Selecting the most stable b-OH conformers at each of the 12 T-sites (T = Si/Al) of H-MFI, a representative set of 26 conformers is obtained which includes free b-OH groups pointing into the empty pore space and b-OH groups forming H-bonds across five- or six-membered rings of TO_4 tetrahedra. Chemically accurate coupled-cluster-quality calculations for periodic models show that the strength of internal H-bonds and, hence, the OH bond length vary substantially with the framework position. For 11 of the 19 H-bonded b-OH groups examined, our predictions fall into the full width at half maximum range of the experimental signals at $3250 \pm 175\ cm^{-1}$ and 7.0 ± 1.4 ppm which supports previously debated assignments of these signals to H-bonded b-OH sites.

Acidic zeolites are crystalline microporous aluminosilicates in which protons balance the negative charge introduced by aluminum atoms in the zeolite framework. They are extensively used in heterogeneous catalysis,[1] e.g., for cracking of hydrocarbons[2] or the methanol-to-olefin process.[3] Among over 230 known framework types, the industrially relevant Socony Mobil-5 (MFI, ZSM5) is one of the most studied in academia.[4]

[*] H. Windeck,[+] Dr. F. Berger,[+] Prof. Dr. J. Sauer
Department of Chemistry, Humboldt-University Berlin
10099 Berlin (Germany)
E-mail: js@chemie.hu-berlin.de

H. Windeck[+]
Department of Interface Science, Fritz Haber Institute of the Max Planck Society
14195 Berlin (Germany)

Prof. Dr. J. Sauer
Department of Physical and Macromolecular Chemistry and Charles University Center of Advanced Materials, Charles University
12843 Prague (Czech Republic)

[+] These authors contributed equally to this work.

Bridging hydroxyl (b-OH) groups, Si–O(H)–Al,[5] are the main source of Brønsted acidity in zeolite catalysts. In the orthorhombic MFI structure,[6] aluminum substitution can occur in 12 crystallographically unique T-sites. The distribution of b-OH groups over different regions of the framework (straight channel, zigzag channel, intersection) influences catalytic properties due to varying confinement (shape selectivity), see, e.g., ref. [7]. However, the distribution of aluminum over the available sites cannot fully be controlled and is subject to active research.[8] ^{27}Al nuclear magnetic resonance (NMR) studies suggest that the aluminum distribution is not random but varies between samples depending on the synthesis conditions.[9]

Infrared (IR) and NMR studies suggest multiple proton sites in H-MFI. Besides the well-established unperturbed, free b-OH groups,[5,10] other signals have been assigned to H-bonded b-OH groups,[11] but often also to defect sites,[12] residual water,[13] H-bonded silanols,[14] or $Al(OH)_n(H_2O)$ species at the external surface.[15] Free b-OH groups cause an OH stretching vibration at around $3600\ cm^{-1}$ and a ^1H NMR chemical shift at around 4 ppm.[10b,c] Kazansky and co-workers reported another, rather broad IR band at $3250\ cm^{-1}$ and tentatively assigned it to H-bonded b-OH groups.[11a] Later, Haw and co-workers[11b] as well as Brunner et al.[11c] reported ^1H NMR chemical shifts at 6.9 and 7.0 ppm, respectively. From a structural analysis, Koller and co-workers inferred that H-bond formation is possible for a significant share of b-OH positions in H-MFI.[16] Conclusive evidence for the existence of such H-bonded b-OH groups has been produced for IFR type zeolites.[17] For H-MFI, the existence of H-bonded b-OH groups has been addressed in previous hybrid QM:MM[18] and QM:QM[19] computational studies (QM = quantum mechanics; MM = molecular mechanics) which, however, remained qualitative due to method limitations, see Table S1 in the Supporting Information.

Here we provide compelling computational evidence for the existence of H-bonded b-OH groups in the framework of H-MFI. We identify eleven H-bonded b-OH groups at different aluminum sites and predict OH vibrational wavenumbers and ^1H NMR chemical shifts that are within the full width at half maximum (FWHM) range of the experimental signals at $3250 \pm 175\ cm^{-1}$ and 7.0 ± 1.4 ppm, respectively.[11c] For free b-OH groups, all predicted IR and ^1H NMR signals are within the FWHM range of the experimental values at $3614 \pm 30\ cm^{-1}$ and 4.2 ± 0.4 ppm, respectively,[11c] demonstrating the accuracy of our calculations.

This level of accuracy is achieved by employing a hybrid QM:QM method[20] for the calculation of energies, forces, and vibrational wavenumbers. The hybrid approach combines density functional theory (DFT) using the Perdew Burke Ernzerhof (PBE) functional[21] and the D2 dispersion term[22] for the full periodic system with second-order Møller Plesset perturbation theory (MP2)[23] for cluster models (MP2:PBE+D2).[20a] As PBE+D3 has no advantage over PBE+D2 for the systems studied here,[22b] we stay with the latter. MP2 yields accurate structures for H-bonded systems, e.g., water clusters.[24] However, to obtain chemically accurate relative stabilities (± 4 kJ mol^{-1}) for H-bonded systems, corrections using coupled cluster with single, double, and perturbative triple substitutions (CCSD(T))[25] need to be added to the hybrid MP2:PBE+D2 energies (MP2:(PBE+D2)+ΔCC).[20a,26] The computational settings have been thoroughly tested, see section 3.1 of the Supporting Information. We provide evidence for the necessity to go beyond the standard approach in computational catalysis, i.e., the use of dispersion-corrected DFT with generalized gradient approximation-type functionals such as PBE+D2 or PBE+D3, see section 3.2 of the Supporting Information.

In H-MFI, four unique b-OH isomers exist for each aluminum site. Moreover, multiple conformers can occur for a given b-OH isomer due to H-bonding with different Si–O–Si acceptor sites, resulting in around 100 b-OH conformers of three different types: b-OH groups pointing into empty pore space (free) and b-OH groups forming H-bonds across five- or six-membered rings of TO_4 tetrahedra (T=Si, Al), HB^{5T} and HB^{6T}, respectively, see Figure 1. Figure S7 in the Supporting Information shows the T-site positions within the MFI framework. Selecting the most stable b-OH conformers at each T-site, a representative set of 26 b-OH conformers is obtained. Table 1 shows their calculated IR and ^{1}H NMR spectroscopic features, for details see section 3.4 of the Supporting Information. A correlation between OH bond lengths and OH stretching wavenumbers is observed, in accordance with Badger's rule,[27] see section 3.3 of the Supporting Information.

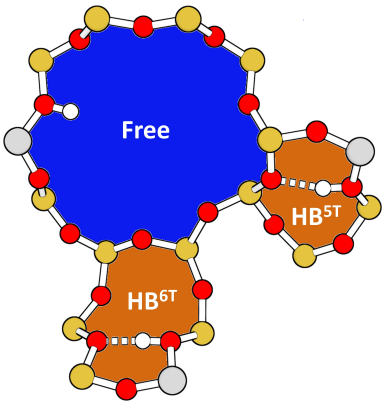

Figure 1. Types of b-OH groups in H-MFI with protons pointing into empty pore space (free) or forming H-bonds (HB) across 5T or 6T rings. Color code: silicon—yellow, aluminum—gray, oxygen—red, and hydrogen—white.

Overall, the selection of sites shown in Table 1 is very diverse, containing free and H-bonded b-OH groups in all regions of the MFI framework which often exhibit similar stability, indicating a compensation of stabilizing H-bond formation and destabilizing framework distortion. This balanced situation with co-existing free and H-bonded b-OH groups is only obtained with our hybrid, coupled cluster quality MP2:(PBE+D2)+ΔCC method. PBE+D2, in contrast, is strongly biased towards H-bonded b-OH groups, see section 3.2 of the Supporting Information for details.

Figure 2 compares the calculated spectroscopic features with the results of Brunner et al.,[11c] who measured IR and ^{1}H NMR spectra for the same H-MFI sample whereas multiple other studies report either IR or ^{1}H NMR spectra of H-MFI. Moreover, the results of Brunner et al.[11c] are selected because the ^{1}H NMR measurements were performed at a particularly low temperature (123 K). This is relevant because the ^{1}H NMR signals of b-OH protons are temperature-dependent[13] and our calculations of spectroscopic features do not take temperature effects into account. Hence, we provide an accurate computational reference for low temperature measurements. Brunner et al. have also performed the IR measurements at low temperature (77 K).[11c] Table S2 in the Supporting Information provides an overview over other experimental IR and ^{1}H NMR values for b-OH groups in H-MFI.

In accordance with previous reports,[29] there is a linear correlation between OH vibrational wavenumbers and ^{1}H NMR shifts. The calculated IR and ^{1}H NMR features for all free b-OH groups are within the FWHM range of the experimental values at 3614 ± 30 cm^{-1} and 4.2 ± 0.4 ppm,[11c] deviating only by 0 to 14 cm^{-1} and −0.3 to 0.4 ppm from the experimental peak maxima, respectively.[11c] Whereas all selected free b-OH groups have similar spectroscopic characteristics, the calculated values for H-bonded b-OH groups cover a broad range of vibrational wavenumbers and

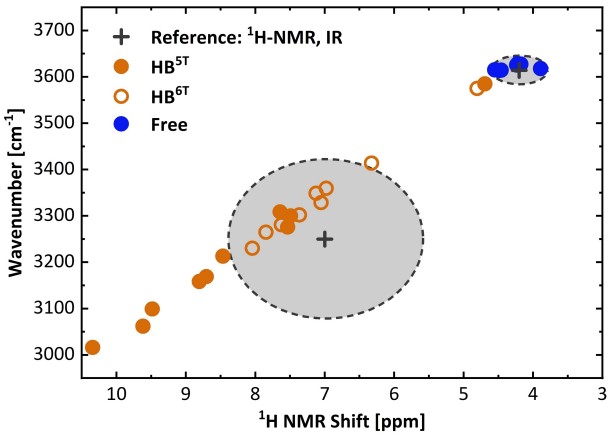

Figure 2. Scaled MP2:PBE+D2 wavenumbers of OH stretching vibrations and cluster-based MP2 ^{1}H NMR chemical shifts of the 26 selected b-OH conformers categorized into free (blue) and H-bonded (orange) b-OH groups within 5T (filled dots) and 6T (empty dots) rings. The scaling factor for wavenumbers is 0.9424, see Table S9 in the Supporting Information. Gray areas indicate the full widths at half maximum range of the experimental values adopted from ref. [11c].

Table 1: MP2 quality results for the most stable b-OH conformers at each aluminum site: MP2:PBE + D2 optimized OH bond lengths (R_{OH}) in pm, MP2:PBE + D2 scaled wavenumbers of OH stretching vibrations (ν_{OH}) in cm^{-1}, cluster-based MP2 ^{1}H NMR chemical shifts (δ_H) in ppm, and their deviations from experimental results (ref. [11c]), $\Delta\nu_{OH}$ and $\Delta\delta_H$, respectively. Coupled cluster quality enthalpies relative to the respective most stable b-OH conformer at each aluminum site (ΔH) at 298 K in kJ mol^{-1} calculated with MP2:(PBE + D2) + ΔCC (MP2:PBE + D2 zero point energies and thermal corrections).

	Position	Site[a]	Type	ΔH	R_{OH}	ν_{OH}[b]	$\Delta\nu_{OH}$	δ_H[c]	$\Delta\delta_H$
Exp.	–	–	Free	–	–	3614	–	4.2	–
	–	–	HB	–	–	3250	–	7.0	–
T1	Al1–O2(H)–Si2	I	Free	0	96.5	3628	14	4.2	0.0
	Al1–O3(H)–Si10	I	HB^{6T}	1	98.1	3329	79	7.1	0.1
T2	Al2–O7(H)–Si6[d]	Z	HB^{5T}	–	98.9	3169	−81	8.7	1.7
T3	Al3–O9(H)–Si4	Z	HB^{5T}	0	99.5	3016	−234	10.3	3.3
	Al3–O5(H)–Si2	I	Free	4	96.6	3615	1	4.6	0.4
T4	Al4–O4(H)–Si1	W	HB^{5T}	–	99.3	3062	−188	9.6	2.6
T5	Al5–O12(H)–Si4	I	HB^{6T}	–	97.7	3414	164	6.3	−0.7
T6	Al6–O10(H)–Si3–(A)[e]	S	HB^{5T}	0	99.2	3099	−151	9.5	2.5
	Al6–O10(H)–Si3–(B)[e]	S	HB^{5T}	9	98.4	3300	50	7.5	0.5
T7	Al7–O17(H)–Si8–(A)[e]	I	Free	0	96.5	3626	12	4.2	0.0
	Al7–O17(H)–Si8–(B)[e]	I	HB^{6T}	0	98.2	3302	52	7.4	0.4
	Al7–O11(H)–Si4[d,e]	Z	Free	4	96.6	3615	1	4.5	0.3
T8	Al8–O6(H)–Si2	S	HB^{5T}	0	98.2	3309	59	7.6	0.6
	Al8–O19(H)–Si9	I	HB^{6T}	3	96.9	3575	325	4.8	−2.2
	Al8–O17(H)–Si7	I	HB^{6T}	4	98.2	3349	99	7.1	0.1
	Al8–O20(H)–Si12	W	HB^{5T}	12	98.4	3276	26	7.5	0.5
T9	Al9–O22(H)–Si10	W	HB^{5T}	0	98.9	3159	−91	8.8	1.8
	Al9–O19(H)–Si8	S	HB^{5T}	2	96.8	3585	335	4.7	−2.3
T10	Al10–O24(H)–Si11	Z	HB^{6T}	0	98.3	3265	15	7.8	0.8
	Al10–O23(H)–Si10	I	Free	1	96.6	3614	0	4.5	0.3
T11	Al11–O14(H)–Si5	S	HB^{5T}	0	98.8	3213	−37	8.5	1.5
	Al11–O24(H)–Si10	Z	HB^{6T}	0	98.5	3281	31	7.6	0.6
	Al11–O16(H)–Si7	I	Free	8	96.6	3618	4	3.9	−0.3
	Al11–O25(H)–O12	I	HB^{6T}	8	98.2	3359	109	7.0	0.0
T12	Al12–O25(H)–Si11	I	HB^{6T}	0	98.5	3230	−20	8.0	1.0
	Al12–O8(H)–Si3	I	Free	1	96.5	3627	13	4.2	0.0

[a] The b-OH conformers can be located in a straight channel (S), zigzag channel (Z), intersection region (I), or wall site (W). [b] scaling factor: 0.9424, see Table S9 in the Supporting Information; [c] reference: tetramethylsilane, internal standard:[28] methanol, see section 1.3 of the Supporting Information for details; [d] see also ref. [18a] and Table S1 in the Supporting Information, [e] see also ref. [19] and Table S1 in the Supporting Information.

chemical shifts, indicating that H-bonds of different strength can be formed. For 11 of 19 H-bonded b-OH groups, our predictions fall into the FWHM range of the experimental signals at $3250 \pm 175\ cm^{-1}$ and 7.0 ± 1.4 ppm.[11c] This is strong evidence for the presence of various H-bonded b-OH groups in H-MFI, in agreement with the conclusions of Koller and co-workers.[16] We do not exclude that extra-framework or partially framework-bound aluminum oxo-hydroxo[12] or other OH defect species like H-bonded silanols[14] or $Al(OH)_n(H_2O)$ sites at the external surface[15] may also contribute to the observed IR and ^{1}H NMR signals depending on the specific H-MFI sample. For a few H-bonded b-OH sites of the HB^{5T} type with aluminum at the T3, T4, and T6 positions, the predictions lie far outside the FWHM range of the experimental values. The absence of the corresponding signals in experimental spectra suggests that these b-OH sites are very rare or absent in the H-MFI samples investigated, considering that the intensity (dipole moment change) of OH stretching modes would increase with increasing wavenumber shift.[30]

In H-MFI, we find H-bonded b-OH groups in 5T and 6T rings and both can explain experimental spectroscopic signals, see Figure 2. On average, H-bonds in 5T rings are stronger than in 6T rings, as indicated by a larger red-shift of the predicted OH vibrational wavenumbers and a down-field-shift of the predicted ^{1}H NMR signals. The reason is that the framework oxygen atoms involved in H-bonds are usually closer to the b-OH proton in 5T rings than in 6T rings, see Tables S13–S48 in the Supporting Information. Previously, evidence for H-bonded b-OH groups has been produced for the zeolite SSZ-42 (IFR framework), attributing ^{1}H NMR peaks at 5.2 and 6.4 ppm to weakly and strongly H-bonded b-OH groups, respectively.[17a] Consistent with our observation for H-MFI, the H-bonds in SSZ-42 are stronger in 5T than in 6T rings.[17a]

Our method is further validated by results for the zeolite chabazite (H-CHA) in which all framework aluminum sites are crystallographically equivalent.[31] As the aluminum atoms are connected to four crystallographically unique oxygen atoms, the CHA framework allows for the formation of four different b-OH isomers. Based on MP2:(PBE + D2) + ΔCC relative enthalpies (298 K), we predict the Al–O4(H)–Si (O4, IZA nomenclature[4c]) b-OH isomer to be most stable, with the Al–O1(H)–Si (O1), Al–O2(H)–Si

(O2), and Al–O3(H)–Si (O3) b-OH isomers being less stable by 3, 14, and 9 kJ mol^{-1}, respectively. Further, we obtain MP2:PBE+D2 OH vibrational wavenumbers of 3599, 3595, 3598, and 3617 cm^{-1} as well as MP2 ^{1}H-NMR chemical shifts of 4.5, 4.3, 4.5 and 4.4 ppm for the O1, O2, O3, and O4 b-OH isomers, respectively, see also Table S10 in the Supporting Information. Experimental IR spectra of H-CHA feature a low-wavenumber band at 3579 cm^{-1} and a high-wavenumber band at 3603 cm^{-1}.[32] Based on our calculations, we assign the O4 b-OH isomer to the high-wavenumber band and the O1, O2, and O3 b-OH isomers to the low-wavenumber band, in accordance with ref. [33]. Due to its relative stability, we expect the O4 b-OH isomer to be predominant. This is in line with the observation that the integrated peak area of the high-wavenumber band is larger than that of the low-wavenumber band.[34] Finally, all calculated ^{1}H-NMR shifts agree within ±0.1 ppm with an observed peak at 4.4 ppm.[35]

In summary, we use a chemically accurate, coupled cluster quality method to find probable b-OH conformers for all aluminum sites of H-MFI and we calculate MP2 level IR and ^{1}H NMR spectroscopic features for this selection. We obtain free and H-bonded b-OH groups. The H-bond strength varies substantially with the framework position, resulting in a wide spread of predicted IR and ^{1}H NMR signals. Our predictions fall into the FWHM range of the experimental IR and ^{1}H NMR signals at 3614 ± 30 cm^{-1} and 4.2 ± 0.4 ppm for free b-OH groups as well as at 3250 ± 175 cm^{-1} and 7.0 ± 1.4 ppm for H-bonded b-OH groups.[11c] This provides compelling evidence that the signals[11c] observed at 3250 cm^{-1} and 7.0 ppm can originate from H-bonded b-OH groups in the H-MFI framework.

Acknowledgements

This work has been supported by German Research Foundation (DFG) with a Reinhart Koselleck grant to J.S., the Fonds der Chemischen Industrie, and by the Charles University Centre of Advanced Materials (CUCAM, OP VVV Excellent Research Teams, project number CZ.02.1.01/0.0/0.0/15_003/0000417). H.W. is member of the International Max Planck Research School for Elementary Processes in Physical Chemistry and holds a Kekulé Fellowship of the Fonds der Chemischen Industrie. F.B. is indebted to the German Academic Scholarship Foundation for a fellowship. Kaido Sillar, University of Tartu, is acknowledged for discussions and the North German Supercomputing Alliance (HLRN) for computer time (grant bec00241). Open Access funding enabled and organized by Projekt DEAL.

Conflict of Interest

The authors declare no conflict of interest.

Data Availability Statement

The data that support the findings of this study are available in the Supporting Information of this article.

Keywords: Brønsted-Acid Sites · IR Spectroscopy · NMR Spectroscopy · MFI · Zeolites

[1] P. Del Campo, C. Martínez, A. Corma, *Chem. Soc. Rev.* **2021**, *50*, 8511–8595.
[2] Y. V. Kissin, *Catal. Rev.* **2001**, *43*, 85–146.
[3] C. D. Chang, *Catal. Rev.* **1983**, *25*, 1–118.
[4] a) R. J. Argauer, G. R. Landolt (Mobil Oil Corp), US3702886A, **1972**; b) K. Tanabe, W. F. Hölderich, *Appl. Catal. A* **1999**, *181*, 399–434; c) C. Baerlocher, L. B. McCusker, "Database of Zeolite Structures", can be found under http://www.iza-structure.org/databases/, **2017**, (accessed 1 March 2023).
[5] W. J. Mortier, J. Sauer, J. A. Lercher, H. Noller, *J. Phys. Chem.* **1984**, *88*, 905–912.
[6] H. van Koningsveld, *Acta Crystallogr. Sect. B* **1990**, *46*, 731–735.
[7] T. Yokoi, H. Mochizuki, T. Biligetu, Y. Wang, T. Tatsumi, *Chem. Lett.* **2017**, *46*, 798–800.
[8] B. C. Knott, C. T. Nimlos, D. J. Robichaud, M. R. Nimlos, S. Kim, R. Gounder, *ACS Catal.* **2018**, *8*, 770–784.
[9] a) S. Sklenak, J. Dědeček, C. Li, B. Wichterlová, V. Gábová, M. Sierka, J. Sauer, *Angew. Chem. Int. Ed.* **2007**, *46*, 7286–7289; b) O. H. Han, C.-S. Kim, S. B. Hong, *Angew. Chem. Int. Ed.* **2002**, *41*, 469–472.
[10] a) G. Engelhardt, H. G. Jerschkewitz, U. Lohse, P. Sarv, A. Samoson, E. Lippmaa, *Zeolites* **1987**, *7*, 289–292; b) D. Freude, M. Hunger, H. Pfeifer, *Z. Phys. Chem.* **1987**, *152*, 171–182; c) P. A. Jacobs, W. J. Mortier, *Zeolites* **1982**, *2*, 226–230.
[11] a) V. L. Zholobenko, L. M. Kustov, V. Y. Borovkov, V. B. Kazansky, *Zeolites* **1988**, *8*, 175–178; b) L. W. Beck, J. L. White, J. F. Haw, *J. Am. Chem. Soc.* **1994**, *116*, 9657–9661; c) E. Brunner, K. Beck, M. Koch, L. Heeribout, H. G. Karge, *Microporous Mesoporous Mater.* **1995**, *3*, 395–399.
[12] a) M. Abdolrahmani, K. Chen, J. L. White, *J. Phys. Chem. C* **2018**, *122*, 15520–15528; b) K. Chen, M. Abdolrahmani, S. Horstmeier, T. N. Pham, V. T. Nguyen, M. Zeets, B. Wang, S. Crossley, J. L. White, *ACS Catal.* **2019**, *9*, 6124–6136; c) K. Chen, M. Abdolrhamani, E. Sheets, J. Freeman, G. Ward, J. L. White, *J. Am. Chem. Soc.* **2017**, *139*, 18698–18704; d) K. Chen, S. Horstmeier, V. T. Nguyen, B. Wang, S. P. Crossley, T. Pham, Z. Gan, I. Hung, J. L. White, *J. Am. Chem. Soc.* **2020**, *142*, 7514–7523.
[13] H. Huo, L. Peng, C. P. Grey, *J. Phys. Chem. C* **2009**, *113*, 8211–8219.
[14] C. Schroeder, V. Siozios, M. Hunger, M. R. Hansen, H. Koller, *J. Phys. Chem. C* **2020**, *124*, 23380–23386.
[15] a) L. Treps, C. Demaret, D. Wisser, B. Harbuzaru, A. Méthivier, E. Guillon, D. V. Benedis, A. Gomez, T. de Bruin, M. Rivallan, L. Catita, A. Lesage, C. Chizallet, *J. Phys. Chem. C* **2021**, *125*, 2163–2181; b) L. Treps, A. Gomez, T. de Bruin, C. Chizallet, *ACS Catal.* **2020**, *10*, 3297–3312.
[16] C. Schroeder, V. Siozios, C. Mück-Lichtenfeld, M. Hunger, M. R. Hansen, H. Koller, *Chem. Mater.* **2020**, *32*, 1564–1574.
[17] a) C. Schroeder, S. I. Zones, M. R. Hansen, H. Koller, *Angew. Chem. Int. Ed.* **2022**, *61*, e202109313; b) L. A. Villaescusa, P. A. Barrett, M. Kalwei, H. Koller, M. A. Camblor, *Chem. Mater.* **2001**, *13*, 2332–2341.

[18] a) U. Eichler, M. Brändle, J. Sauer, *J. Phys. Chem. B* **1997**, *101*, 10035–10050; b) M. Sierka, J. Sauer, *J. Phys. Chem. B* **2001**, *105*, 1603–1613.
[19] K. Sillar, P. Burk, *J. Phys. Chem. B* **2004**, *108*, 9893–9899.
[20] a) J. Sauer, *Acc. Chem. Res.* **2019**, *52*, 3502–3510; b) C. Tuma, J. Sauer, *Chem. Phys. Lett.* **2004**, *387*, 388–394.
[21] J. P. Perdew, K. Burke, M. Ernzerhof, *Phys. Rev. Lett.* **1996**, *77*, 3865–3868.
[22] a) S. Grimme, *J. Comput. Chem.* **2006**, *27*, 1787–1799; b) F. R. Rehak, G. Piccini, M. Alessio, J. Sauer, *Phys. Chem. Chem. Phys.* **2020**, *22*, 7577–7585.
[23] C. Møller, M. S. Plesset, *Phys. Rev.* **1934**, *46*, 618–622.
[24] J. A. Anderson, K. Crager, L. Fedoroff, G. S. Tschumper, *J. Chem. Phys.* **2004**, *121*, 11023–11029.
[25] G. D. Purvis III, R. J. Bartlett, *J. Chem. Phys.* **1982**, *76*, 1910–1918.
[26] a) F. Berger, J. Sauer, *Angew. Chem. Int. Ed.* **2021**, *60*, 3529–3533; b) Q. Ren, M. Rybicki, J. Sauer, *J. Phys. Chem. C* **2020**, *124*, 10067–10078.
[27] a) R. M. Badger, *J. Chem. Phys.* **1934**, *2*, 128–131; b) K. R. Asmis, G. Meijer, M. Brümmer, C. Kaposta, G. Santambrogio, L. Wöste, J. Sauer, *J. Chem. Phys.* **2004**, *120*, 6461–6470.
[28] F. Haase, J. Sauer, *J. Am. Chem. Soc.* **1995**, *117*, 3780–3789.
[29] a) M. Sierka, U. Eichler, J. Datka, J. Sauer, *J. Phys. Chem. B* **1998**, *102*, 6397–6404; b) H. Kriegsmann, *Z. Phys. Chem.* **1988**, *269O*, 178–180.
[30] C. M. Huggins, G. C. Pimentel, *J. Phys. Chem.* **1956**, *60*, 1615–1619.
[31] L. S. Dent, J. V. Smith, *Nature* **1958**, *181*, 1794–1796.
[32] L. J. Smith, A. Davidson, A. K. Cheetham, *Catal. Lett.* **1997**, *49*, 143–146.
[33] P. M. Kester, J. T. Crum, S. Li, W. F. Schneider, R. Gounder, *J. Catal.* **2021**, *395*, 210–226.
[34] S. Bordiga, L. Regli, D. Cocina, C. Lamberti, M. Bjørgen, K. P. Lillerud, *J. Phys. Chem. B* **2005**, *109*, 2779–2784.
[35] B. A. Aufdembrink, D. P. Dee, P. L. McDaniel, T. Mebrahtu, T. L. Slager, *J. Phys. Chem. B* **2003**, *107*, 10025–10031.

Manuscript received: March 3, 2023
Version of record online: May 9, 2023